



Enhanced hydrogen sorption properties in the $\text{LiBH}_4\text{-MgH}_2$ system catalysed by Ru nanoparticles supported on multiwalled carbon nanotubes

Jianfeng Mao^a, Zaiping Guo^{a,b,*}, Xuebin Yu^{c,a,**}, Huakun Liu^a

^a Institute for Superconducting and Electronic Materials, University of Wollongong, Wollongong, NSW 2522, Australia

^b School of Mechanical, Materials & Mechatronics Engineering, University of Wollongong, Wollongong, NSW 2522, Australia

^c Department of Materials Science, Fudan University, Shanghai 200433, China

ARTICLE INFO

Article history:

Received 20 December 2010

Received in revised form 31 January 2011

Accepted 2 February 2011

Available online 27 February 2011

Keywords:

Hydrogen storage

MgH_2

LiBH_4

Catalysis

Carbon-supported Ru nanoparticles

ABSTRACT

The $\text{LiBH}_4\text{-MgH}_2$ system has a high reversible hydrogen storage capacity. However, the hydrogen de/absorption kinetics has to be further enhanced for its practical application. Motivated by the possibility that the metal catalysts facilitating the dissociation and combination of hydrogen molecules and activating Mg–H and B–H bonds, a novel catalyst, ruthenium nanoparticles supported on multiwalled carbon nanotubes (Ru/C) is prepared and its effect on the hydrogen sorption properties of $\text{LiBH}_4\text{-MgH}_2$ systems is investigated. The experimental results show that the Ru/C catalyst is active in reducing the dehydrogenation temperature and enhancing the dehydrogenation kinetics. Furthermore, the reversible capacity is also markedly enhanced under moderate conditions, and the catalytically enhanced hydrogen absorption capacity persists well during three de/rehydrogenation cycles.

© 2011 Elsevier B.V. All rights reserved.

1. Introduction

Metal borohydrides are of interest for hydrogen storage in mobile applications due to their high gravimetric and volumetric densities of hydrogen [1]. However, the strong covalent bonding between B and H in the BH_4 unit makes them too stable with respect to thermal decomposition. For example, LiBH_4 has a large theoretical hydrogen capacity of 18.5 wt.% in the family of metal borohydrides, and is considered to be a promising hydrogen storage material for mobile application [2]. However, high temperatures are required to obtain the useful hydrogen capacity, approximately 380 °C for the main evolution of gas to start, and only half of the hydrogen can be released below 600 °C [3,4]. Recently, a variety of additives have been screened, and some were found to be effective in lowering the thermodynamics and kinetics [5–8]. However, the conditions of rehydrogenation of LiBH_4 are still very high, which may be attributed to the general chemical inertness of boron, which is hard to be activated due to the strong boron–boron bonds [3]. An effective method developed by Vajo et al. [9] and Barkhordarian et al. [10], independently, was to use MgH_2 to modify the de/rehydrogenation thermodynamics

of LiBH_4 through forming MgB_2 compound upon dehydrogenation according to $\text{LiBH}_4 + \text{MgH}_2 \leftrightarrow \text{LiH} + \text{MgB}_2 + 4\text{H}_2$. The mixture of $2\text{LiBH}_4 + \text{MgH}_2$ has good reversibility under relatively moderate conditions in the presence of 3 mol% TiCl_3 [9]. It was suggested that MgB_2 promotes the formation of the BH_4 complex, as the activation energy needed to break the Mg–B bond is lower than that of the B–B bond [10,11]. However, the reaction kinetics of the $2\text{LiBH}_4 + \text{MgH}_2$ mixture was still slow. For example, 100 h is needed to attain equilibrium for direct measurements, even at 400 °C [9]. Furthermore, the reversibility still needs further improvement in order to make the system suitable as an on-board hydrogen storage medium in mobile applications.

In an effort to develop the $\text{LiBH}_4\text{-MgH}_2$ system with improved dehydrogenation kinetics and reversibility, we focus on catalyst screening to catalytically enhance the reversible dehydrogenation of the $\text{LiBH}_4\text{-MgH}_2$ system. It has been well established that metallic catalysts may facilitate the dissociation and combination of hydrogen molecules and consequently improve de/absorption kinetics of metal hydrides or complex hydrides. For example, it has been reported that Ru-based catalysts possess pronounced catalytic activity for the activation of N–H bond and the dissociative chemisorption of hydrogen molecule [12,13]. In this regard, the Ru-based catalysts may also be active toward the de/rehydrogenation of MgH_2 and LiBH_4 . On the other hand, it has also been well known that with a small curvature radius, carbon exhibits prominent “catalytic” effect in conventional metal hydrides and complex hydrides [14]. In the present study, the effect of ruthenium metallic nanoparticles sup-

* Corresponding authors at: Institute for Superconducting and Electronic Materials, University of Wollongong, NSW 2522, Australia.

** Corresponding authors at: Department of Materials Science, Fudan University, Shanghai 200433, China.

E-mail addresses: zguo@uow.edu.au (Z. Guo), yuxuebin@fudan.edu.cn (X. Yu).

ported on multiwalled carbon nanotubes (Ru/C) on the hydrogen de/absorption properties of $\text{LiBH}_4\text{-MgH}_2$ system is systematically investigated.

2. Experimental

2.1. Preparation of Ru/C catalyst

The MWNTs were first prepared by catalytic chemical vapor deposition (CVD), using nanosized cobalt as the catalyst [15]. The MWNTs were firstly treated in concentrated HNO_3 at 393 K for 2 h. Then, the mixture was diluted with water, filtered, washed with excess deionized water, and dried at 60 °C in a vacuum oven. After that Ru–MWNTs (Ru/C) catalysts were prepared by microwave heating of an ethyleneglycol (EG) solution of $\text{RuCl}_3 \cdot x\text{H}_2\text{O}$ with MWNTs suspended in the solution. A typical preparation would consist of the following steps: 400 mg pretreated MWNTs, 15 ml of 0.05 M $\text{RuCl}_3 \cdot x\text{H}_2\text{O}$ (Aldrich, A.C.S. Reagent) in EG solution, and 30 ml of 0.04 M KOH were mixed with 100 ml of EG (Aldrich) in a beaker and ultrasonicated with an ultrasonic probe for 4 h. The beaker were placed in the center of the microwave oven and heated for 2 min under a microwave power of 800 W, at that point Ru particles were reduced from the solution [16,17]. The as-prepared suspension was filtered, and the residue was washed with acetone and de-ionized water. Finally, the prepared Ru/C catalyst was dried under vacuum at room temperature.

2.2. Preparation of $\text{LiBH}_4\text{-MgH}_2$ samples

The starting materials MgH_2 (98% purity) and LiBH_4 (95% purity) were purchased from Sigma–Aldrich Co. and used directly without pretreatment. A mixture of $2\text{LiBH}_4 + \text{MgH}_2$ with 10 wt.% Ru/C added was ball milled for 2 h at a rate of 400 rpm in a QM-2SP planetary ball mill. The ball-to-powder ratio was around 30:1. For comparison purposes, the $2\text{LiBH}_4 + \text{MgH}_2$ mixture without Ru/C was also ball milled and examined under the same conditions. All sample storage and handling were performed in an Ar filled glove box (MBraun Unilab).

2.3. Property measurements and structural characterization

The hydrogen desorption/absorption properties were measured in a Sieverts apparatus (Advanced Materials Corporation, USA). Temperature programmed dehydrogenation (TPD) curves were determined by volumetric methods, starting from static vacuum. The temperature was increased from ambient to ~500 °C at 2 °C/min. The hydrogen desorption kinetic measurements were performed at the desired temperature starting from static vacuum. Before the onset of kinetic measurement, the sample chamber was filled with hydrogen at 4 MPa pressure, and the temperature was then raised to and kept at the desired temperature. Then, the chamber was quickly evacuated. The hydrogen absorption measurements were performed at about 4 MPa and 500 °C. The sample was thoroughly dehydrogenated at 500 °C under dynamic vacuum before the rehydrogenation measurement. Other than specified, the hydrogen capacity calculations were normalized to the $\text{LiBH}_4\text{-MgH}_2$ content, aiding comparison between samples with and without additive.

The Ru/C catalysts were characterized by using scanning electron microscopy (SEM, JEOL JSM-6460A) equipped with an energy dispersive spectrometer (EDS). Transmission electron microscopy (TEM) was performed using a JEOL JEM 2011. TEM samples were dispersed on lacey carbon support films. The $\text{LiBH}_4\text{-MgH}_2$ samples with Ru/C catalyst were analysed using X-ray diffraction (XRD, Rigaku D/max 2200PC, $\text{Cu K}\alpha$ radiation). In order to avoid the possible oxidation during the XRD measurement, samples were mounted onto a glass board 1 mm in thickness in the Ar filled glove box and sealed with an airtight hood composed of an amorphous tape.

3. Results and discussion

3.1. Catalyst characterization

It is well known that MWNTs have a hydrophobic surface, which results in aggregation in polar solvent. Therefore, it is necessary to functionalize the surface of MWNTs by acid treatment in order to facilitate the deposition of a large amount of Ru nanoparticles with uniform distribution. Typical SEM images of as-prepared Ru/C catalysts are shown in Fig. 1a. It can be seen that Ru nanoparticles (bright spots) are uniformly distributed among the MWNTs. Fig. 1b presents a typical EDS pattern of the as-prepared Ru/C catalyst, which indicates the presence of Ru. The amount of Ru nanoparticles loaded on the MWNT support was also estimated by semi-quantitative EDS, and it was found that the Ru nanoparticles are about 20 wt.% of the total composites for Ru–MWNT.

The general distribution of Ru nanoparticles on the surfaces of the MWNTs is further characterized by TEM as shown in Fig. 2. It can

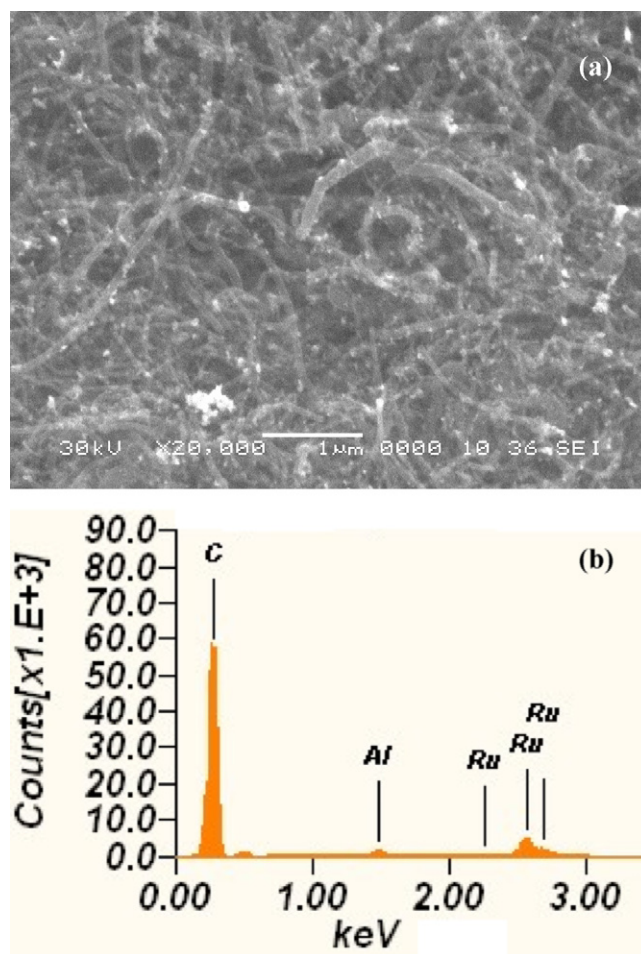


Fig. 1. (a) SEM image of the as-prepared Ru/C catalyst, and (b) EDS patterns of the Ru/C catalyst.

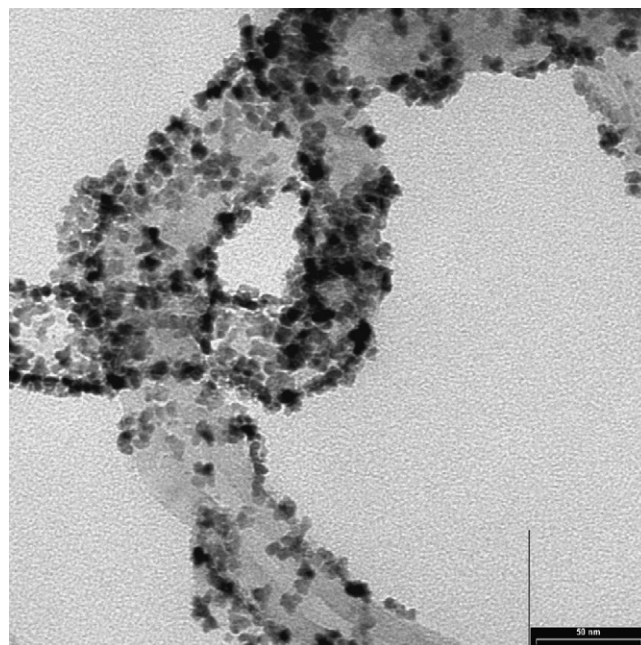


Fig. 2. TEM image of the as-prepared Ru/C catalyst.

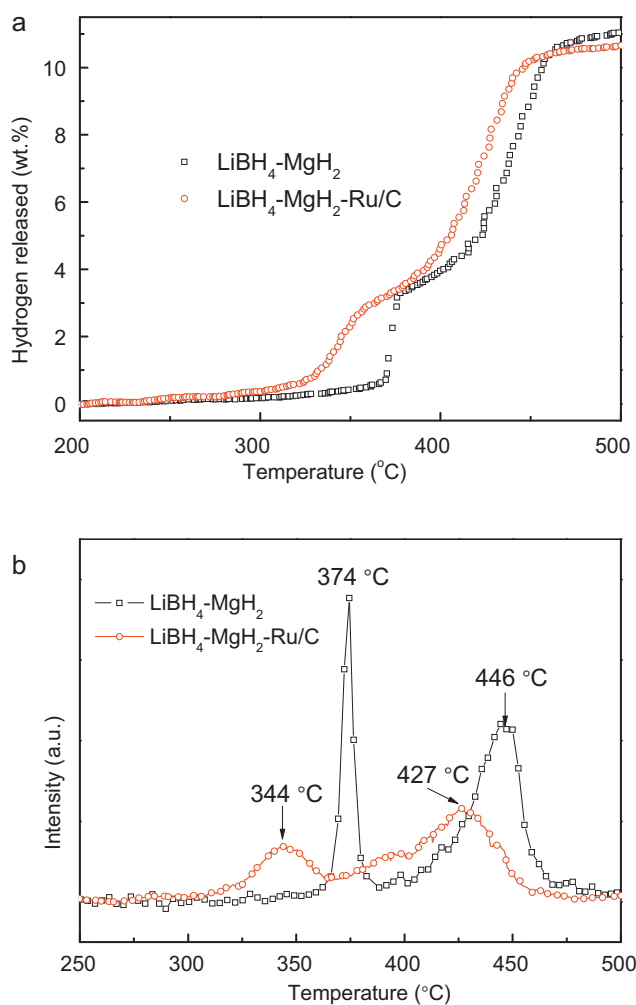


Fig. 3. (a) TPD (temperature-programmed desorption), and (b) derivative temperature-programmed desorption (DTPD) curves of 2 h ball milled $\text{LiBH}_4\text{-MgH}_2$ mixtures with and without catalyst addition. The heating ramp for all the samples was $2^\circ\text{C}/\text{min}$.

be seen that the surfaces of the MWNTs were uniformly decorated by Ru nanoparticles with an average particle sizes range from 2 to 5 nm.

3.2. Hydrogen de/absorption and catalytic mechanistic study of the Ru-catalyzed $\text{LiBH}_4\text{-MgH}_2$ material

Property examination shows that the Ru/C catalyst is effective for enhancing the hydrogen desorption of the $2\text{LiBH}_4 + \text{MgH}_2$ material. Fig. 3 presents the temperature-programmed desorption curves and the differentiated (DTPD) curves for the dehydrogenation of undoped and Ru/C doped $\text{LiBH}_4\text{-MgH}_2$ samples. It can be seen that both the doped and undoped samples showed a clear two-step dehydrogenation, which corresponds to the decomposition of MgH_2 and LiBH_4 , respectively, with increasing temperature. From the TPD results (Fig. 3a), we can find that the first hydrogen desorption for the undoped sample started at around 360°C . Further heating led to a second dehydrogenation starting at around 380°C , and a total hydrogen release capacity of 11 wt.% was obtained by 500°C . After doping with Ru/C, the system started to release hydrogen at around 310°C , and reached its second-step hydrogen release process at 360°C , which is 50°C and 20°C lower than for the undoped sample, respectively. Meanwhile, two main peaks of hydrogen evolution located at 374 and 446°C can be observed in

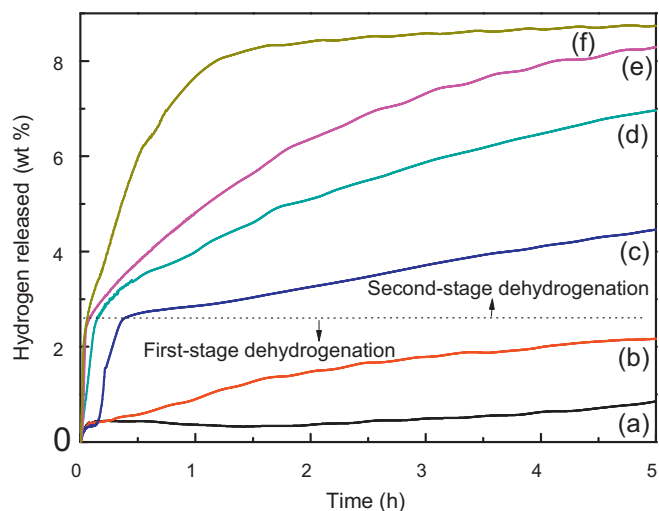


Fig. 4. Hydrogen desorption curves of the plain $\text{LiBH}_4\text{-MgH}_2$ system at 300 (a), 350 (c), and 380°C (e). Hydrogen desorption curves of the Ru/C catalyzed $\text{LiBH}_4\text{-MgH}_2$ system at 300 (b), 350 (d), and 380°C (f).

the TPD results (Fig. 3b). After doping with Ru/C, the peak temperature for the first and second dehydrogenation of the doped sample is 344 and 427°C , which is 30 and 19°C , respectively, lower than for the undoped sample. These results indicate the dehydrogenation properties of $\text{LiBH}_4\text{-MgH}_2$ were improved by Ru/C catalyst doping.

In order to judge the dehydrogenation kinetics of Ru/C catalyzed $\text{LiBH}_4\text{-MgH}_2$ sample, isothermal dehydrogenation was studied at 300 , 350 , and 380°C , respectively, as shown in Fig. 4. The dehydrogenation kinetics of pure $\text{LiBH}_4\text{-MgH}_2$ sample is also examined for comparison. It can be seen that there are two stages in the dehydrogenation process for the two samples at 350 and 380°C : fast dehydrogenation in the first short period, corresponding to the decomposition of MgH_2 , and slow dehydrogenation thereafter, which results from the dehydrogenation of LiBH_4 . The figure also shows that the dehydrogenation process for the Ru/C doped $\text{LiBH}_4\text{-MgH}_2$ sample is saturated with a capacity of 8.39 wt.% within 2 h at 380°C , while only 6.37 wt.% hydrogen was released for the undoped sample under the same conditions and the dehydrogenation is still proceeding even after 5 h. At 350°C , the undoped sample only released 4.45 wt.% hydrogen within 5 h, which is much lower than that of the doped sample (6.98%). At 300°C , the hydrogen release is mainly attributed to the dehydrogenation of MgH_2 in both samples, in which only 0.83 wt.% of hydrogen was released from the undoped sample after 5 h, while 2.2 wt.% of hydrogen was released from the Ru/C doped sample. These results indicate that the dehydrogenation kinetics of the $\text{LiBH}_4\text{-MgH}_2$ system is significantly improved by doping Ru/C. Particularly, the catalytically enhanced kinetics arising upon adding Ru/C catalyst is achieved without penalty of the practical capacity of the materials, indicating that the added catalyst activates more $2\text{LiBH}_4 + \text{MgH}_2$ component to participate in the dehydrogenation reaction at these temperatures.

The addition of Ru/C catalyst was also highly effective for improving the rehydrogenation process in the $\text{LiBH}_4\text{-MgH}_2$ system under more moderate conditions. Fig. 5 compares the rehydrogenation kinetics of the neat and Ru/C catalyzed systems under the initial pressure of 4 MPa H_2 at 500°C . Clearly, the enhanced rehydrogenation kinetics and increased hydrogen recharging amount were observed in the Ru/C catalyzed sample. In the case of the Ru/C catalyzed sample, a hydrogen absorption capacity of 5.4 wt.% was reached in 2 h. Furthermore, the sample can absorb 7.5 wt.% hydrogen within 8 h, which is 2.2 wt.% higher than that of the neat sample under the same conditions.

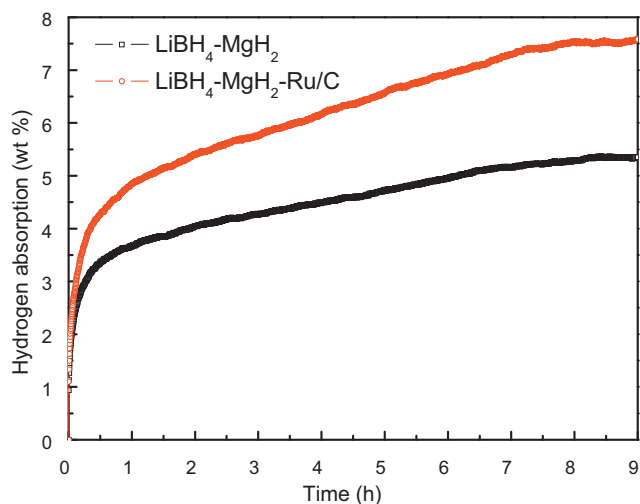


Fig. 5. Comparison of hydrogen absorption curves for the un-catalyzed and catalyzed $\text{LiBH}_4\text{-MgH}_2$ system at 500°C under 4 MPa hydrogen.

Further study indicates that the Ru/C catalyzed sample have good de/rehydrogenation cyclic properties. Fig. 6 compares the rehydrogenation capacity of the neat and Ru/C catalyzed systems under the initial pressure of 4 MPa H_2 at 500°C for 9 h. As shown in Fig. 5, the rehydrogenation capacity of the Ru/C catalyzed sample at the first and the third cycle are almost the same, 7.8 wt.% in the first cycle, and 7.6 wt.% after three cycles. In contrast, the rehydrogenated capacity for the neat sample is reduced from 5.8 wt.% for the first cycle to 5.4 wt.% for the third cycle. The well persisted rehydrogenation capacity in Ru/C catalyzed sample indicates that the Ru/C catalyst has a good catalytic activity even after several cycling.

Fig. 7 shows the XRD patterns of the as-prepared Ru/C catalyzed $\text{LiBH}_4\text{-MgH}_2$ system and of the same sample after dehydrogenation and subsequent rehydrogenation. After ball milling, the sample showed the characteristics of a physical mixture of MgH_2 and LiBH_4 , but no peaks related to the catalyst were observed due to the much lower concentration and nanocrystalline phase. However, after heating to 500°C , the MgH_2 and LiBH_4 peaks were absent, and new compounds, corresponding to Mg, Li–Mg alloy, LiH, and some MgB_2 (with Li–Mg alloy and Mg peaks overlapping in the XRD patterns), were observed. The decomposition product of B from LiBH_4 is suggested to be amorphous state, and therefore, cannot

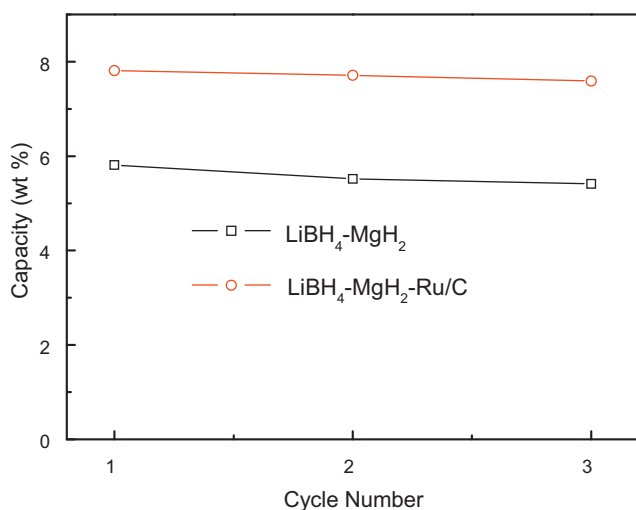


Fig. 6. The rehydrogenation cycling of the un-catalyzed and Ru/C catalyzed $\text{LiBH}_4\text{-MgH}_2$ system at 500°C under 4 MPa hydrogen.

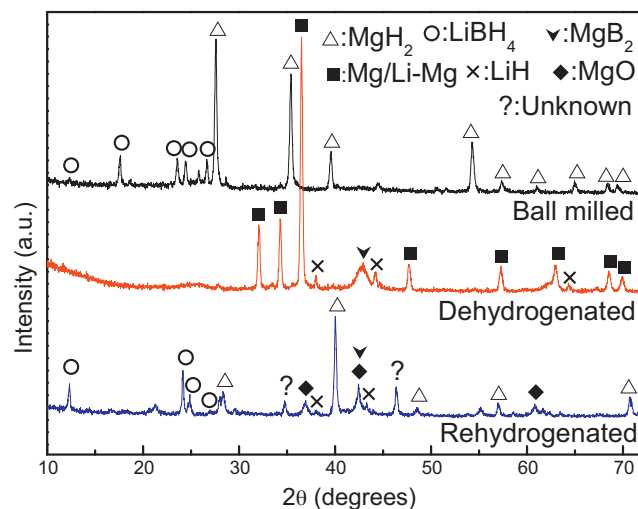


Fig. 7. XRD patterns of the Ru/C catalyzed $\text{LiBH}_4\text{-MgH}_2$ system: as-milled; after dehydrogenation at 500°C ; and after the first rehydrogenation at 500°C under 4 MPa hydrogen.

be detected. The results are in good agreement with the previous report, in which the formation of MgB_2 is suggested to use hydrogen back-pressure above 3 bar upon dehydrogenation [18]. It is also suggested that the formation of MgB_2 , rather than B, might promote the rehydrogenation reaction, as it requires much less energy to break Mg–B bonding in MgB_2 compared to the B–B bonding in the bulk B [4]. It has also already been reported that mixtures of $\text{LiH} + 1/2\text{MgB}_2$ including 2–3 mol% TiCl_3 can reversibly store 8–10 wt.% hydrogen from an initial hydrogen pressure of 100 bar, beginning at $230\text{--}250^\circ\text{C}$ for 10 h [9]. Meanwhile, Yu et al. [19] have shown that the dehydrogenated $\text{LiBH}_4\text{-MgH}_2$ can be rehydrogenated without the formation of MgB_2 at 400°C under 100 bar hydrogen pressure. In this regard, the reversibility of the reaction does not depend on the formation of MgB_2 under high temperature and hydrogen pressure conditions. Here, our results show that the Ru/C catalyzed $\text{LiBH}_4\text{-MgH}_2$ system could reversibly absorb hydrogen under more moderate conditions. As shown in Fig. 7, MgH_2 and LiBH_4 are clearly reformed from the dehydrogenated products under conditions of 500°C and 4 MPa H_2 for 9 h. It is believed that the Ru/C catalyst plays an important role in improving the rehydrogenation kinetics of the $\text{LiBH}_4\text{-MgH}_2$ system by reducing the activation barriers for the hydrogenation reaction. However, full rehydrogenation in the Ru/C catalyzed $\text{LiBH}_4\text{-MgH}_2$ system is still not reached under these moderate conditions, which may be due to the strong boron–boron bonds in elemental boron ($\Delta H_{\text{B(s)}\rightarrow\text{B(g)}} = 560\text{ kJ/mol}$), resulting in high kinetic barriers [4]. In this regard, a study on the effect of the application of hydrogen back-pressure during the dehydrogenation should be conducted and the effect on the subsequent rehydrogenation under moderate conditions. In addition, MgO was also detected in the rehydrogenation state due to the slight oxygen contamination from the XRD measurement or hydrogenation process, which may result in a decrease of the cycled capacity.

Combined utilization of the catalytically active metal nanoparticles and nanostructured carbon materials to improve the dehydrogenating/rehydrogenating properties of metal hydrides has been intensely developed over the past several decades, where the carbon nanotubes are expected to form a net-like structure after being milled together with host metal hydrides, thus creating a micro-confined environment for the decomposition/restoration of hydrides, while the metal nanoparticles have high catalytic activity. For example, the hydrogen storage properties of MgH_2 are significantly enhanced by introducing carbon nanotubes and metal

particles [20–22]. Furthermore, the carbon nanotubes and particles of metals such as Pt, Pd, and Ni are also effective in catalytically enhancing the reversible dehydrogenation of LiBH_4 [23–27]. Particularly, Wang et al. [28] reported that the reversible dehydrogenation properties of $\text{LiBH}_4\text{--MgH}_2$ system could be considerably improved by mechanically milling with different carbon additives. In this regard, as a source of metal nanoparticles and carbon nanotubes, the as-prepared Ru/C provides an ideal choice for catalysing the dehydrogenation/rehydrogenation of the $\text{LiBH}_4\text{--MgH}_2$ system. Further efforts will focus on the enhancement of the dehydrogenation kinetics and full reversibility under more moderate conditions by using hydrogen back-pressure and optimizing the structure and composition of the metal based catalysts.

4. Conclusions

In summary, the hydrogen de/absorption properties of the $\text{LiBH}_4\text{--MgH}_2$ system were improved by introducing the Ru nanoparticles distributed on the MWNTs support. Compared to the neat $\text{LiBH}_4\text{--MgH}_2$ system, the samples containing Ru/C catalyst exhibit considerable enhancement on the dehydrogenation/rehydrogenation kinetics. Also, a reversible rehydrogenation capacity of ~ 7.8 wt.% has been demonstrated under moderate conditions (500°C , 4 MPa) for 9 h, which is 2 wt.% higher than for the neat system. Moreover, the catalytically enhanced rehydrogenation capacity arising upon adding Ru/C catalyst is highly stable during de/rehydrogenation cycling. The result is encouraging for pursuing $\text{LiBH}_4\text{--MgH}_2$ as a mixture with considerable potential as a reversible hydrogen storage medium by screening more highly active heterogeneous metal catalysts.

Acknowledgements

This work has been supported by an Australian Research Council (ARC) Discovery project (DP0878661), and the National Natural Science Foundation of China (51071047). The authors are also grateful to Dr. Tania Silver from University of Wollongong for her kind correction on the writing.

References

- [1] S. Orimo, Y. Nakamori, J.R. Eliseo, A. Züttel, C.M. Jensen, *Chem. Rev.* 107 (2007) 4111–4132.
- [2] L. Schlapbach, A. Züttel, *Nature* 414 (2001) 353.
- [3] A. Züttel, S. Rentsch, P. Fischer, P. Wenger, P. Sudan, P. Mauron, C. Emmenegger, *J. Alloys Compd.* 356–357 (2003) 515–520.
- [4] S. Orimo, Y. Nakamori, G. Kitahara, K. Miwa, N. Ohba, S. Towata, A. Züttel, *J. Alloys Compd.* 404–406 (2005) 427–430.
- [5] J. Yang, A. Sudik, C. Wolverton, *J. Phys. Chem. C* 111 (2007) 19134–19140.
- [6] M. Au, A. Jurgensen, *J. Phys. Chem. B* 110 (2006) 7062–7067.
- [7] M. Au, A. Jurgensen, W. Spencer, D. Anton, F.E. Pinkerton, S. Hwang, C. Kim, R. Bowman, *J. Phys. Chem. C* 112 (2008) 18661–18671.
- [8] X.B. Yu, D.M. Grant, G.S. Walker, *J. Phys. Chem. C* 113 (2009) 17945–17949.
- [9] J.J. Vajo, S.L. Skeith, F. Mertens, *J. Phys. Chem. B* 109 (2005) 3719–3722.
- [10] G. Barkhordarian, T. Klassen, M. Dornheim, R. Bormann, *J. Alloys Compd.* 440 (2007) L18–L21.
- [11] J.F. Mao, Z.P. Guo, Y.Y. Leng, Z. Wu, Y.H. Guo, X.B. Yu, H.K. Liu, *J. Phys. Chem. C* 114 (2010) 11643–11649.
- [12] L. Li, Z.H. Zhu, Z.F. Yan, G.Q. Lu, L. Rintoul, *Appl. Catal. A Genet.* 320 (2007) 166–172.
- [13] L.P. Ma, H.B. Dai, Y. Liang, X.D. Kang, Z.Z. Fang, P.J. Wang, P. Wang, H.M. Cheng, *J. Phys. Chem. C* 112 (2008) 18280–18285.
- [14] C.Z. Wu, H.M. Cheng, *J. Mater. Chem.* 20 (2010) 5390–5400.
- [15] Z.P. Guo, Z.W. Zhao, H.K. Liu, S.X. Dou, *Carbon* 43 (2005) 1392–1399.
- [16] Z.P. Guo, D.M. Han, D. Wexler, R. Zeng, H.K. Liu, *Electrochim. Acta* 53 (2008) 6410–6416.
- [17] D.M. Han, Z.P. Guo, Z.W. Zhao, R. Zeng, Y.Z. Meng, D. Shu, H.K. Liu, *J. Power Sources* 184 (2008) 361–369.
- [18] F.E. Pinkerton, M.S. Meyer, G.P. Meisner, M.P. Balogh, J.J. Vajo, *J. Phys. Chem. C* 111 (2007) 12881–12885.
- [19] X.B. Yu, D.M. Grant, G.S. Walker, *Chem. Commun.* 37 (2006) 3906–3908.
- [20] C.X. Shang, Z.X. Guo, *J. Powder Sources* 129 (2004) 73–80.
- [21] C.Z. Wu, P. Wang, X.D. Yao, C. Liu, D.M. Chen, G.Q. Lu, H.M. Cheng, *J. Alloys Compd.* 414 (2006) 259–264.
- [22] X.D. Yao, C.Z. Wu, A.J. Du, et al., *J. Am. Chem. Soc.* 129 (2007) 15650–15654.
- [23] X.B. Yu, Z. Wu, Q. Chen, Z. Li, B. Weng, T. Huang, *Appl. Phys. Lett.* 90 (2007) 034106.
- [24] Z.Z. Fang, X.D. Kang, P. Wang, H.M. Cheng, *J. Phys. Chem. C* 112 (2008) 17023–17029.
- [25] G.L. Xia, Y.H. Guo, Z. Wu, X.B. Yu, *J. Alloys Compd.* 479 (2009) 545–548.
- [26] J. Xu, J. Cao, Z. Zou, D.L. Akins, H. Yang, *J. Alloys Compd.* 490 (2010) 88–92.
- [27] J. Xu, X.B. Yu, J. Ni, Z. Zou, Z. Li, H. Yang, *Dalton Trans.* 39 (2009) 8386–8391.
- [28] P.J. Wang, Z.Z. Fang, L.P. Ma, X.D. Kang, P. Wang, *Int. J. Hydrogen Energy* 35 (2010) 3072–3075.